Journal of Photochemistry and Photobiology A: Chemistry 279 (2014) 52–58

Contents lists available at ScienceDirect

Journal of Photochemistry and Photobiology A: Chemistry

journal homepage: www.elsevier.com/locate/jphotochem

Photophysical behaviour of 4-hexyloxysalicylaldimies and their copper(II) complexes

William A. Greenbank, Kathryn M. McGrath*

MacDiarmid Institute for Advanced Materials and Nanotechnology, School of Chemical and Physical Sciences, Victoria University of Wellington, Wellington, New Zealand

ARTICLE INFO

Article history:
Received 2 July 2013
Received in revised form 22 January 2014
Accepted 24 January 2014
Available online 5 February 2014

Keywords:
Alkoxysalicylaldimine
Enol-imine tautomers
Photochromism
Electronic absorption spectroscopy
Density functional theory

ABSTRACT

Salicylaldimines are popular ligands used in the synthesis of anisotropic complexes which can form liquid crystal phases (metallomesogens). They tautomerise *via* exchange of the phenol proton, giving rise to solvent-dependent photophysical behaviour. In this study the photophysical behaviour of a family of 4-alkoxysalicylaldimine ligands and their corresponding copper(II) complexes were examined using electronic absorption spectroscopy and density functional theory (DFT). The solvent-dependent photophysical behaviour exhibited by the ligands is due to changes in the position of the tautomeric equilibrium as the degree of hydrogen-bonding character of the solvent is modified. Furthermore, the ligands bind in an intermediate state in the copper(II) complex, with the possible existence of a third tautomer. The electronic absorption properties of these compounds are strongly affected by changes in the environment around the molecule.

1. Introduction

Salicylaldimines (Scheme 1) are popular ligands in transition metal chemistry. In particular, the square planar complexes they form are frequently employed in the synthesis of metallomesogens (metal-containing liquid crystals) as the complexes are highly anisotropic and the ligands are easily modified. Transition metal-salicylaldimine metallomesogens exhibit a range of structure-dependent mesophases, detailed in the review by Hoshino [1].

One well-known feature of salicylaldimines is their ability to tautomerise *via* transfer of the phenol proton (Scheme 1), presenting as the enol-imine or keto-amine tautomer. The enol-imine tautomer has the lower energy. Tautomerization arises due to photoexcitation (photochromism) [2], variation of solvent/complex interactions [3], and thermal excitation [2].

Although the relationships between metallomesogens' chemical structure and their phase behaviour have been thoroughly investigated, comparatively few studies have been made of their physical properties. Previous studies show that the physical properties of the metallomesogen in the mesophase are markedly different from those observed in the crystalline or isotropic states and are highly dependent on the structure of the mesophase [4]. Understanding these relationships is critical to finding new applications for liquid crystals.

Here the photophysical properties of salicylaldimine ligands, differing only in the length of the hydrocarbon chains and the corresponding copper(II) complexes (Scheme 2) were examined using solution phase electronic absorption spectroscopy and compared to results obtained from DFT simulations. The structure of the core of these molecules is commonly used in metallomesogens; variants of these complexes with differing alkyl chain lengths were investigated by Paschke et al. for their liquid crystal properties [5], and the mesogenic properties of the N-phenyl variants (*vide infra*) are reviewed by Hoshino [1]. The electronic properties of these complexes, however, are not well understood, in particular how these properties respond to structural changes and changes in the environment around the molecule; these are the focus of this paper.

In particular we focus on the ability of the solvent to alter the position of the tautomeric equilibrium and how the ligands bind to the copper. This has not been investigated previously. Understanding the electronic behaviour of the ligands when bound to copper and how the environment around the ligands affects their structure and electronic properties is critical in understanding any self-assembly dependent electronic interactions.

2. Methods

2.1. Synthesis

The ligands were synthesised in two steps (Scheme 2). In the first step the alkoxy chain is formed by reaction of 4-hydroxysalicyaldehyde with n-alkylbromide in the presence of

* Corresponding author. Tel.: +64 4 463 5963.
E-mail address: kathryn.mcgrath@vuw.ac.nz (K.M. McGrath).

1010-6030/$ – see front matter © 2014 Elsevier B.V. All rights reserved.
http://dx.doi.org/10.1016/j.jphotochem.2014.01.012

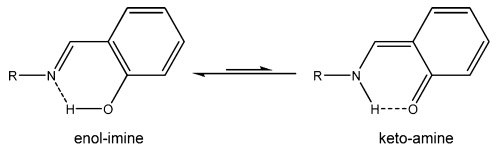

Scheme 1. The tautomerization equilibrium between the enol-imine and keto-amine tautomers of a salicylaldimine.

potassium bicarbonate. In the second step, the imine bond is formed *via* condensation with either 1-aminoalkane to form the L1 series of ligands (N-alkyl), or 4-alkylaniline to form the L2 ligand series (N-phenyl).

Complexation with copper was achieved by reacting the appropriate ligand with copper(II) acetate. The ligands were characterised using infrared, ultraviolet, and ^{13}C and ^{1}H NMR spectroscopies, while the complexes were characterised by infrared and ultraviolet spectroscopies, and elemental analysis.

Syntheses done under inert atmospheres were carried out by degassing the reaction vessel in nitrogen gas and then fitting the vessel with a balloon of the relevant gas (all supplied by BOC New Zealand).

The synthetic protocols were adapted from: Yelamaggad et al. [6], van Deun and Binnemans [7], Paschke et al. [5], and López de Murillas [8]. A family of ligands and complexes were synthesised (Scheme 2). The hexyl members of the two families are highlighted as exemplars of the ligands and complexes investigated.

2.1.1. 4-Hexyloxysalicylaldehyde

To a solution of 2,4-dihydroxybenzaldehyde (1.08 g, 7.77 mmol, Sigma–Aldrich, 98%) in dry acetone (20 mL, Panreac, ≥99%, ≤0.01% H_2O) were added potassium bicarbonate (789 mg, 7.88 mmol, May and Baker Ltd., ≥98%), and n-hexylbromide (7.80 mmol, Merck, 98%). The mixture was refluxed under an argon atmosphere for 90 hours. The reaction mixture was then filtered through diatomaceous earth. The crude products were purified by flash chromatography, using a 19:1 mixture of petroleum ether/ethyl acetate as the eluent. Yield: 62% of a pale yellow oil. R_f: 0.6 (4:1 petroleum ether/ethyl acetate). ^{1}H NMR (500 MHz, $CDCl_3$): δ 11.48 (s, 1H); 9.70 (s, 1H); 7.41 (d, 8.8 Hz, 1H); 6.52 (dd, 8.8 Hz, 2.3 Hz, 1H); 6.41 (d, 2.2 Hz, 1H); 4.00 (t, 6.6 Hz, 2H); 1.79 (quin., 7.1 Hz, 2H); 1.45 (m, 2H); 1.2–1.4 (m, 4H); 0.91 (t, 7.1 Hz, 3H).

2.1.2. N-hexyl 4-hexyloxysalicylaldimine (L1(6,6))

4-Hexyloxysalicylaldehyde, acetic acid (one equivalent, Pure Science, AR grade–glacial), and 1-aminohexane (1.2 equivalent, Merck, 98%) were dissolved in absolute ethanol (15 mL, Pure Science, ≥98.85%) under a nitrogen atmosphere. The solution was refluxed for four hours under nitrogen. The solvent was removed *in vacuo*, and the crude product was purified by flash chromatography, using a 9:1 mixture of petroleum ether/ethyl acetate as the eluent. Yield: 77% of a viscous yellow oil. R_f: 0.5 (4:1 petroleum ether/ethyl acetate). ^{1}H NMR (500 MHz, $CDCl_3$): δ 14.15 (s, 1H); 8.09 (s, 1H); 7.06 (d, 8.5 Hz, 1H); 6.37 (d, 2.2 Hz, 1H); 6.33 (dd, 8.7 Hz, 2.3 Hz, 1H); 3.96 (t, 6.6 Hz, 2H); 3.52 (t, 6.8 Hz, 2H); 1.78 (quin., 7.1 Hz, 2H); 1.67 (quin., 7.1 Hz, 2H); 1.26–1.48 (m, 12H); 0.91 (t, 6.6 Hz, 3H); 0.90 (t, 6.9 Hz, 3H). ^{13}C NMR (500 MHz, $CDCl_3$): δ 167.7; 163.5; 163.1; 132.5; 111.8; 106.7; 102.0; 68.0; 57.1; 31.6; 31.5; 30.8; 29.0; 26.7; 25.7; 22.6; 22.6; 14.0; 14.0. IR ν/cm^{-1}: 2955 (C—H); 2928 (C—H); 2855 (C—H); 2800 (O—H); 1624 (C=N); 1514 (C—OH).

2.1.3. N-(4-butylphenyl) 4-hexyloxysalicylaldimine (L2(4,6))

The same procedure as above was used, except that 4-butylaniline (1.2 equivalent, Sigma–Aldrich, ≥97%) was used instead of 1-aminohexane. Yield: 94% of a yellow crystalline solid that melts slightly above room temperature to form a cloudy yellow

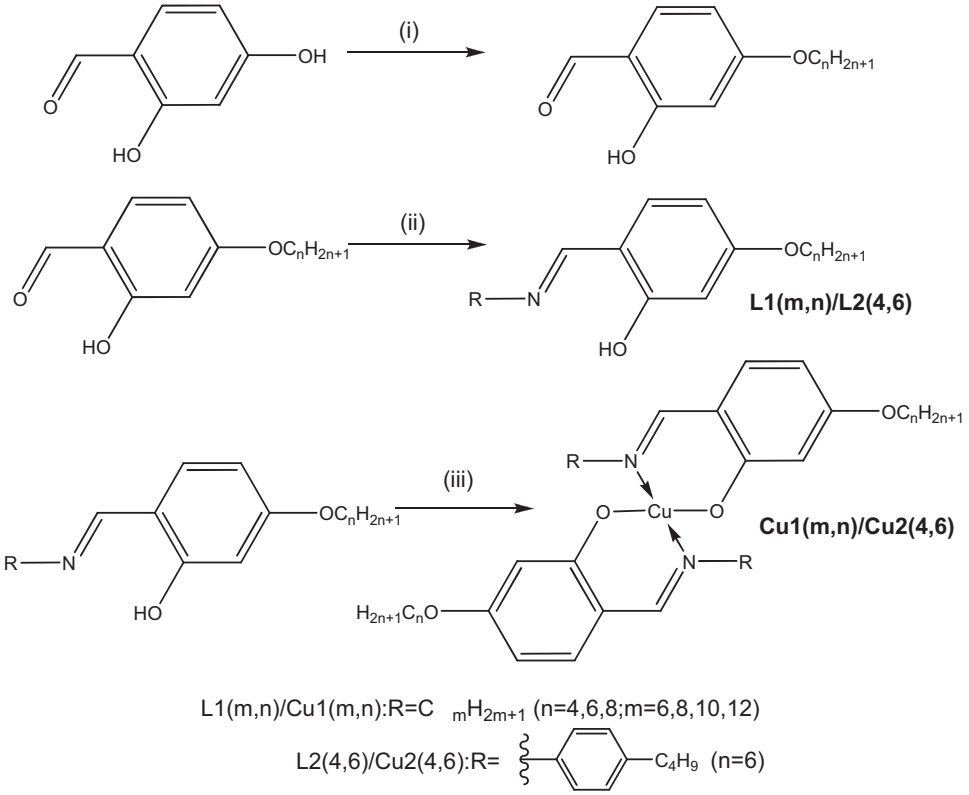

Scheme 2. Reaction scheme: (i) $C_nH_{2n+1}Br$, $KHCO_3$, acetone; (ii) $C_nH_{2n+1}NH_2$/4-butylaniline, AcOH, EtOH; and (iii) $Cu(OAc)_2$, EtOH. L1(6,6), L2(4,6) and their corresponding copper(II) complexes Cu1(6,6) and Cu2(4,6) are discussed in the text as examples.

Table 1
Solvents used in electronic absorption experiments.

Solvent	Supplier	Purity
Acetonitrile	Panreac	99.9%
Ethanol (absolute)	Pure Science	≥98.85%
n-Hexane	Labscan	99%
Methanol (dry)	Panreac	99.8%, ≤0.005% H_2O

fluid. R_f: 0.5 (4:1 petroleum ether/ethyl acetate). ^{1}H NMR (500 MHz, $CDCl_3$): 13.94 (s, 1H); 8.52 (s, 1H); 7.24 (d, 8.3 Hz, 1H); 7.21 (d, 8.5 Hz, 2H); 7.18 (d, 8.0 Hz, 2H); 6.49 (s, 1H); 6.47 (d, 8.5 Hz, 1H); 4.00 (t, 6.6 Hz, 2H); 2.63 (t, 7.8 Hz, 2H); 1.80 (quin., 7.5 Hz, 2H); 1.61 (quin., 7.6 Hz, 2H); 1.3–1.5 (m, 8H); 0.94 (t, 7.6 Hz, 3H); 0.92 (t, 7.0 Hz, 3H). ^{13}C NMR (500 MHz, $CDCl_3$): δ 164.0; 163.5; 160.6; 145.9; 141.3; 133.3; 129.3; 120.8; 113.0; 107.5; 101.6; 68.2; 35.2; 33.7; 31.6; 29.0; 25.7; 22.6; 22.3; 14.0; 14.0. IR ν/cm^{-1}: 2958 (C—H); 2956 (C—H); 2859 (C—H); 2750 (O—H); 1618 (C=N); 1598 (C=N); 1514 (C—OH).

2.1.4. Bis (N-hexyl 4-hexyloxysalicylaldimine) copper(II) (Cu1(6,6))

A solution of L1(6,6) (2.0 mmol) in absolute ethanol (10 mL) was added dropwise to a stirring solution of copper(II) acetate monohydrate (1.0 mmol, May and Baker Ltd., ≥98.5%) in absolute ethanol (10 mL) at 60 °C. The mixture was refluxed for five hours before being allowed to cool to room temperature overnight. Following this, the solvent was removed *in vacuo* and the resulting green solid was dissolved in dichloromethane (Panreac, ≥99.9%) and filtered through diatomaceous earth. The dichloromethane was removed *in vacuo* and the remaining solid was recrystallised from absolute ethanol. Yield: 80% of a golden crystalline solid. IR ν/cm^{-1}: 2957 (C—H); 2932 (C—H); 2857 (C—H); 1605 (C=N); 1527 (C—OCu). Anal. Calc. for $CuC_{38}H_{60}N_2O_4$: C 67.87, H 8.99, N 4.17; Found: C 68.18, H 9.31, N 4.20%.

2.1.5. Bis (N-(4-butylphenyl) 4-hexyloxysalicylaldimine) copper(II) (Cu2(4,6))

The same procedure as outlined in 2.1.4 was used, with L2(4,6) (2.0 mmol) replacing L1(6,6). Yield: 54% of a golden crystalline solid. IR ν/cm^{-1}: 2954 (C—H); 2931 (C—H); 2858 (C—H); 1608 (C=N); 1587 (C=N); 1523 (C—OCu). Anal. Calc. for $CuC_{46}H_{60}N_2O_4$: C 71.89, H 7.87, N 3.65; Cu 8.27; Found: C 72.32, H 8.01, N 3.65; Cu 8.3%.

2.2. Instrumentation

NMR spectra were obtained in deuterated chloroform (Sigma–Aldrich, 99.8% atom D, 17.6 ppm H_2O) using a Varian Unity Inova 500 spectrometer. Infrared spectra were obtained using a Bruker Tensor 27 FTIR spectrometer in attenuated total reflectance (ATR) mode and elemental analysis was carried out by the Campbell Microanalytical Laboratory at the University of Otago.

Electronic absorption data were obtained using a Varian Cary 100, dual beam, baseline corrected UV–vis spectrophotometer in transmission mode. Solutions were prepared quantitatively. The solvents used, their suppliers and purities are shown in Table 1.

2.3. Computational methods

Gaussian 09 was used to perform all computations [9]. Geometry optimisation was carried out using DFT with a B3LYP functional and a 6-31G++ basis set in the case of L1(6,6) and 6-31G** in the case of Cu1(6,6). Excited state calculations were performed using time dependent DFT (TD-DFT) with the same functional and basis set. TD-DFT has been used to calculate the excited states of similar compounds previously [10]. Charge distributions were determined by the natural bond orbital (NBO) method [11]. Selected extracted data are supplied in the electronic supplementary data.

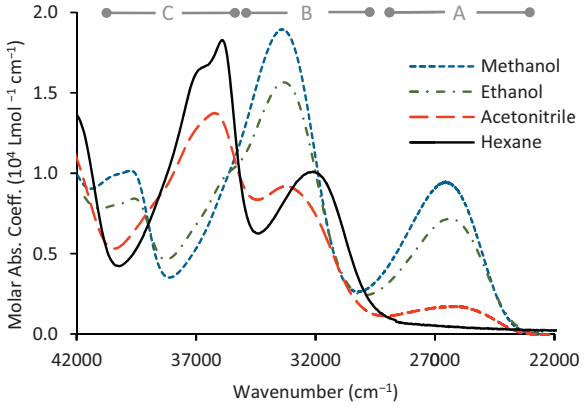

Fig. 1. The electronic absorption spectra of L1(6,6) (representative of L1 ligands) in a range of solvents with bands A, B, and C annotated.

3. Results and discussion

3.1. Photophysical properties of the ligands

The solution phase electronic absorption spectrum of the L1 (N-alkyl) ligands show significant variation with solvent (Fig. 1), but negligible variation with N-alkyl and alkoxy chain lengths. The largest difference is observed for the spectra in hexane and methanol where the band labelled C (Fig. 1) is significantly blue shifted with a decreased intensity. The band labelled B is blue shifted with an increase in intensity. Band A is very weak in hexane and very strong in methanol.

This solvent effect is also seen when ethanol is used (Fig. 1), but is present to a far smaller extent when acetonitrile is used. These data indicate that the effect arises due to the hydrogen-bonding character of the solvents, and not their polarity.

This dependence of the data on the hydrogen-bonding character of the solvent suggests that the solvent effects are the result of a tautomeric equilibrium being established in solution (analogous to that shown in Scheme 1). This is supported by the observation of a highly deshielded ^{1}H NMR resonance of the phenolic proton (14.15 ppm) and the peak broadening brought about by coupling to the nitrogen indicating a high degree of intra-molecular hydrogen-bonding between the two. For the enol-imine (O—H N) the hydrogen bond is 1.725 Å and for the keto-amine (O H—N) 1.714 Å, based on the ground state DFT data.

Hammud et al. proposed that the solvent dependence is due to hydrogen-bonding solvents increasing the acidity of the phenol proton [12], therefore shifting the position of the tautomeric equilibrium more towards the keto-amine tautomer. If this is the driving factor for the L1 ligands, it is expected that features due to the presence of both tautomers in solution would be evident in the spectrum and that quantitative analysis would provide the equilibrium ratios as set by the hydrogen-bonding character of solvent.

Of the solvents shown in Fig. 1, hexane has no hydrogen-bonding character, hence in solution only the enol-imine tautomer will be present. Conversely, methanol has the most hydrogen-bonding character of the solvents and would therefore contain the largest proportion of the keto-amine tautomer. Comparison of the spectra obtained for the L1(6,6) ligand in methanol *vs.* hexane reveals few, if any, common features (it is noted that the breadth of the peaks may mask particular features). When one considers the spectrum obtained in ethanol there is a shoulder at 35,500 cm^{-1} potentially

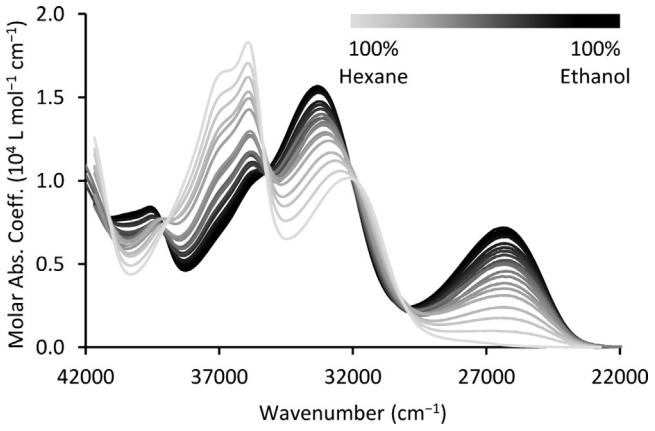

Fig. 2. Titration study of L1(6,6) ligand where the solvent is varied from 100% (v/v) ethanol to 100% (v/v) hexane.

corresponding to the enol-imine tautomer band C. To investigate this further, a titration experiment was performed where the solvent was varied from 100% v/v ethanol to 100% v/v hexane (Fig. 2).

The growth of one peak at the expense of another in the band C region, as well as the presence of multiple isosbestic points, shows that these data result from the presence of two separate chemical species. If the solvent effects were due to the solvent affecting the energy of the ground or excited states of the transition in band C, then a gradual progression of the peak from 35,700 cm^{-1} to 39,200 cm^{-1} would be observed, not the growth of one peak at the expense of the other as seen here. These observations can be rationalised if band C is assigned to a π–π^* transition delocalised over the conjugated system. The reduction in wavelength and molar absorption coefficient would be consistent with the formation of the keto-amine tautomer as this would reduce the extent of conjugation. This assignment is consistent with reported studies of other salicylaldimine-based compounds [12–14].

The behaviour of band B is, at first glance, harder to rationalise by this means. Peaks in this region and having this intensity in the spectra of salicylaldimine compounds are generally assigned to a π–π^* transition localised on the imine C=N chromophore [12–14]. This peak would therefore be expected to decline in intensity as the proportion of the enol-imine tautomer is reduced by the addition of a hydrogen-bonding solvent. This is not consistent with the data shown in Figs. 1 and 2, in which the peak increases significantly in intensity, and shifts to lower wavelength with increasing ethanol fraction.

The inconsistency between the predicted decline in band B and the experimental data can potentially be explained when the chromophores present in the keto-amine tautomer, in particular the ketone formed at the 2 position on the ring are considered. If the π–π^* transition of the ketone is more strongly absorbing than the imine in the enol-imine tautomer, and has a peak wavelength slightly below that of the imine, then the two absorbances would appear as a single peak, especially when the peaks are broad. The apparent growth of the peak with increasing ethanol volume fraction would then be as expected.

Turning now to band A. This band is strongly affected by the hydrogen-bonding character of the solvent and is therefore related to the tautomerism of the ligands. There has been a number of studies of the photochromism of salicylaldimine-based compounds [2,12] in which tautomerization from the enol-imine tautomer to the higher energy keto-amine tautomer is induced by irradiation with ultraviolet radiation. Band A is therefore consistent with such a photochromic charge transfer as it is similar in wavelength to photochromic charge transfer bands in similar compounds [2], and

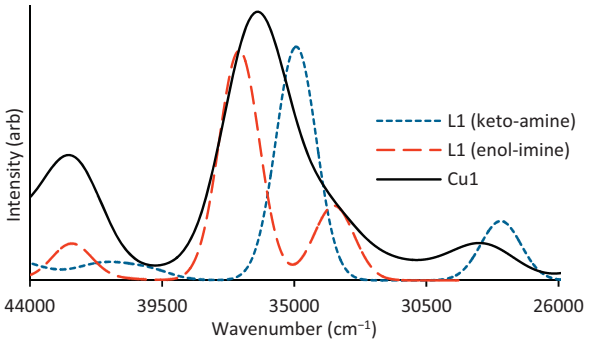

Fig. 3. Simulated electronic absorption spectra of the enol-imine and keto-amine tautomers of the L1(6,6) ligand, and Cu1(6,6) calculated with TD-DFT using Gaussian 09 [9]. Note that the intensities of bands are not comparable between spectra.

because of its strong dependence on the hydrogen-bonding ability of the solvent.

The data for acetonitrile support these conclusions, with its very weak capacity to hydrogen bond. Hence the equilibrium lies predominantly towards the enol-imine and the intensity of band A is very weak though readily observed.

The electronic absorption of the two tautomers of the L1(6,6) ligand was modelled with TD-DFT (Fig. 3, see ESI for full data on molecular orbital energies, symmetries and transitions contributing to the calculated peaks) using the Gaussian 09 software package [9]. The calculated UV–vis spectrum of the enol-imine tautomer shows bands that can be correlated to bands B and C in the spectrum of the L1(6,6) ligand in hexane at 33,700 cm^{-1} and 37,000 cm^{-1} respectively. Likewise, in the calculated spectrum of the keto-amine tautomer, bands at 27,900 cm^{-1}, 35,000 cm^{-1} and 41,500 cm^{-1} can be correlated to bands A, B and C (respectively) in the measured spectrum of the L1(6,6) ligand in methanol. This further supports the hypothesis that the solvent effects observed in the experimental spectra are due to differences in the equilibrium levels of the two tautomers in solvents with different hydrogen-bonding character.

As shown in Fig. 4, the UV–vis spectrum of L2(4,6) contains the same features as those observed and fully discussed above for the L1 ligands. For L2(4,6) the bands are red shifted and there are some differences in intensity. This is consistent with the extended conjugation in the L2(4,6) ligand as compared with the L1 series. Another expected consequence of the extra phenyl ring in L2(4,6) is that bands B and C no longer show the strong solvent dependence exhibited by L1 ligands. This is because of the increased stability of the enol-imine tautomer due to the greater conjugation, hence the tautomeric equilibrium is shifted much further towards the

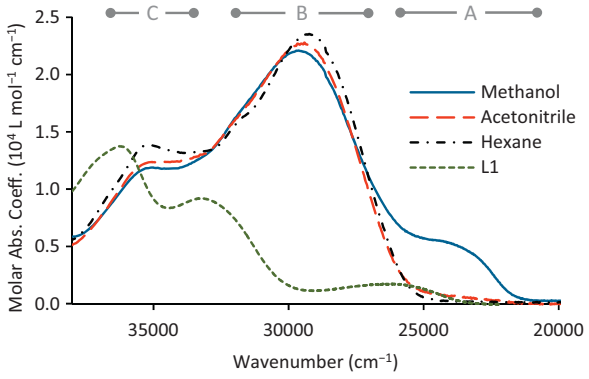

Fig. 4. Electronic absorption spectra of L2(4,6) in a range of solvents with bands A, B and C annotated. The spectrum of the L1(6,6) ligand in acetonitrile is shown for reference (dashed curve).

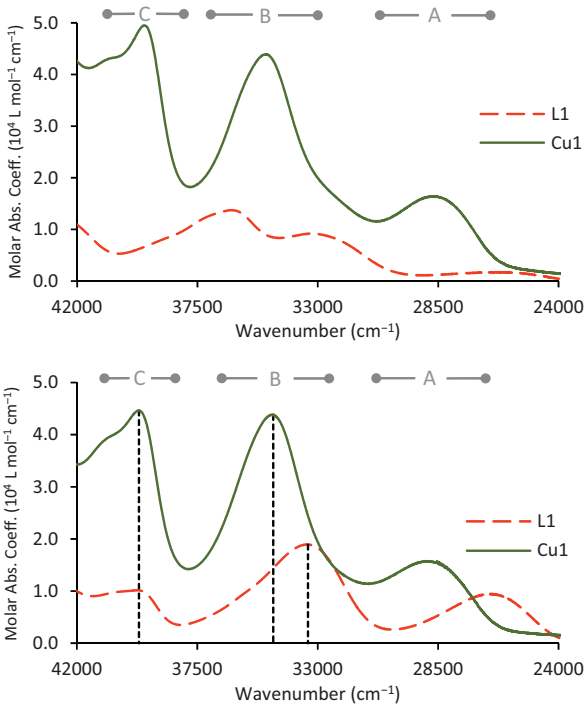

Fig. 5. Representative electronic absorption spectra of the Cu1 complexes in acetonitrile (top) and methanol (bottom), shown here for Cu1(6,6). Bands A, B and C are labelled and the spectra of L1(6,6) are shown for reference, data for the C6 ligand and complex are shown.

enol-imine tautomer. As such solvent effects are significantly reduced. The greatest effect is seen for band A, but this is still significantly reduced compared with the L1 series.

3.2. Photophysical properties of the complexes

Complexation of L1 ligands to copper(II) have two main effects on the electronic absorption spectrum (Fig. 5). The first is that the molar absorption coefficient of all peaks is significantly increased. An increase in the molar absorption coefficients is expected, since the ligands form a 2:1 complex with copper, meaning that the number of chromophores per mole is effectively doubled upon complexation. What is unusual, though, is that for some of the peaks the intensity more than doubles upon complexation. This effect has been reported in previous studies of similar complexes by Paschke et al. [5], Bhattacharjee et al. [13], and Vafazadeh et al. [14], but no attempt was made to explain the results in these reports.

The other noticeable effect is the blue shifts of all the peaks upon complexation. This is reminiscent of the blue shifted peaks of the L1 ligands discussed in Section 3.1. Comparing the methanol spectra of the L1(6,6) ligand and the corresponding copper(II) complex, Cu1(6,6) (Fig. 5), shows that the wavelength of band C matches, and the wavelength of band B is only blue shifted by 1100 cm^{-1} upon complexation. This suggests that the L1 ligands actually favour the keto-amine tautomer when bound to copper in solution, not the enol-imine tautomer which is favoured when not bound.

This also explains the apparent significant increase in the molar absorption coefficient as the intensity of band C in the spectrum of a pure or enriched solution of the keto-amine tautomer of an L1 ligand would be higher than band C in the spectrum of a methanol solution of an L1 ligand as the latter is a mixture of both tautomers with a slight preference for the enol-imine tautomer. The shift in band B can be explained when one considers that band B in the spectrum of an L1 ligand in methanol is a composite of two peaks, one from each tautomer. Therefore the position of band B in the

Table 2
Bond lengths determined from DFT simulations of the L1(6,6) ligand and Cu1(6,6) complex.

	Amine/imine C—N/Å	Ketone/enol C—O/Å
L1(6,6) (keto-amine)	1.326	1.270
Cu1(6,6)	1.301	1.302
L1(6,6) (enol-imine)	1.287	1.345

spectra of the Cu1 series is most likely closer to the position of the component of band B in the L1 series spectra that arises from the keto-amine tautomer.

In addition to the ligand-centred bands, an additional very low intensity, broad peak is evident at 16,100 cm^{-1} (130 L mol^{-1} cm^{-1}). This is due to the metal-centred *d–d* transition and is consistent with other similar compounds [14].

The TD-DFT simulation of the electronic absorption spectrum of the Cu1(6,6) complex (Fig. 5) contains features that can be correlated to bands A, B and C in the measured spectrum. The simulated spectrum contains features from both tautomers, indicating the ligand is in a state that is intermediate to the two tautomers when bound. Moreover, the bond lengths of the amine/imine C—N and ketone/enol C—O bonds in the DFT optimised structure of Cu1(6,6) (Table 2), are between the values for the keto-amine and enol-imine tautomers of L1(6,6).

The hypothesis that the ligand binds to copper(II) in an intermediate state to the two tautomers is also supported by the plot of the HOMO of the DFT optimised Cu1(6,6) complex (Fig. 6). This shows that the aromatic π system is partially delocalised to include both the enol/ketone oxygen and the nitrogen. In addition, the HOMO plot shows that the alkoxy oxygen is included, suggesting involvement of a third tautomer that was not observed in the free ligand. The calculated charge distribution in the complex (calculated using

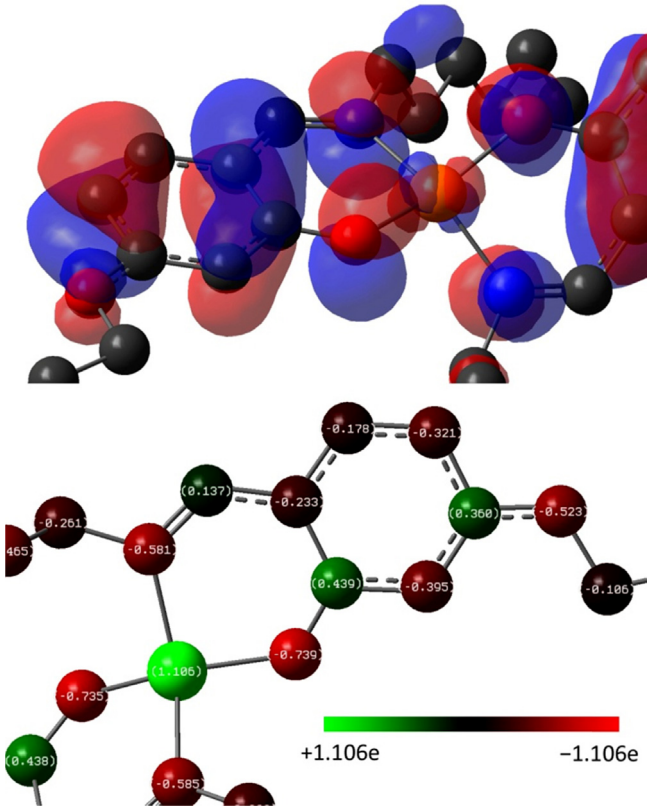

Fig. 6. (Top) A plot of the HOMO of the DFT optimised structure of Cu1(6,6) and (bottom) the charge distribution in the DFT optimised structure of Cu1(6,6) calculated using the NBO method [11].

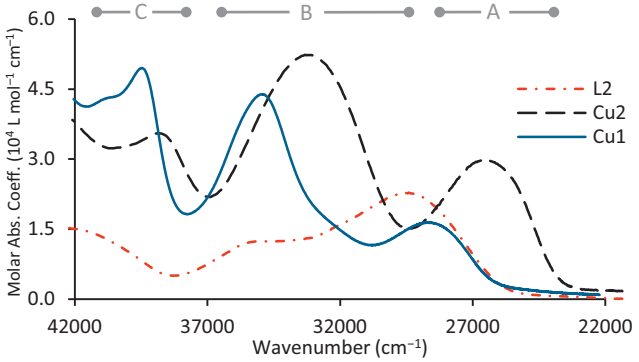

Fig. 7. The electronic absorption spectrum of Cu2(4,6) in acetonitrile with bands A, B and C labelled. The spectra of L2(4,6) and Cu1(6,6) in acetonitrile are shown for reference.

the natural bond orbital method [11]) indicates that this oxygen has a lower charge than the enol/ketone oxygen, suggesting that this tautomer is less favoured than the other two.

The blue shift of band A upon complexation of an L1 ligand to copper(II) is much greater than that for bands B and C. This can be justified when one considers that in the L1 ligands, band A results from a photochromic charge transfer, exciting the molecule into the high energy keto-amine tautomer from the more stable enol-imine tautomer. It is evident that, without a proton to transfer, this tautomerism is no longer possible. Further evidence for this comes from the solvent dependence that was observed for the L1 ligand series which is no longer observed on complexation to copper(II). Since band A in the Cu1 complex spectrum does not originate from photochromism, it must be a new band resulting from complexation to copper. Given its similarity to band A in the L1 ligands spectra, it most likely still arises from a charge transfer, but this time involving the metal rather than a phenol proton, *i.e.* a ligand to metal charge transfer, LMCT. This is consistent with the lack of solvent dependency as the transition does not depend on the lability of a phenol proton as in the case of the ligand. This also agrees with the studies done by Vafazadeh et al. [14] and Tas et al. [15] who reported that bands in this region in similar complexes resulted from LMCT.

The changes in the L2(4,6) data upon complexation to copper(II) are relatively similar to those observed following complexation of the L1 ligands to copper(II) with regard to the blue shift and increase in molar absorption coefficient for peaks B and C for the complex *vs.* the ligand (Fig. 7). This is consistent with the ligands of Cu2(4,6) binding to copper(II) in an intermediate state to the two tautomers, in the same manner as the ligands of Cu1. The molar absorption coefficient of the LMCT band A in Cu2(4,6) is significantly increased compared with the corresponding band in the Cu1 spectra and is red shifted by 2200 cm^{-1}. Since the LMCT transition causes a substantial redistribution of charge in the molecule, increasing the extent of conjugation would be expected to have both of these effects as it would raise the probability of the transition and better stabilise the excited state *via* resonance.

4. Conclusions

In this study we have observed that the L1 and L2 ligand series exhibit strong solvent dependence in their electronic absorption spectra. Through the use of electronic absorption spectroscopy, and TD-DFT simulations, this was shown to be due to the ligands existing in a tautomeric equilibrium. This enables their photophysical properties to be strongly affected by their environment, particularly the presence of any hydrogen-bonding, which is relevant to how the ligands would behave electronically in a mesophase, either as ligands, mesogens or dopants.

This study has also used electronic absorption spectroscopy and TD-DFT simulations to demonstrate for the first time the binding mode of the ligands to copper. The bands of the Cu1 and Cu2 complexes are blue shifted from those of the free ligands. The wavelengths of the ligand-centred bands indicate that the ligands in either complex bind to the metal centre in solution in a form that exhibits features of the keto-amine tautomer, despite the free ligand preferring the lower energy enol-imine tautomer. TD-DFT simulations confirm that the ligands are in a state that is intermediate to the two tautomers, and that aspects of both are present in the electronic absorption spectra of the Cu1 complexes.

The electronic absorption properties of these compounds are strongly affected by changes in the environment around the molecule. This will prove important in understanding any self-assembly dependent photophysical properties that these compounds exhibit.

Acknowledgements

The authors thank Ivan Welsh and Zhi Xiang Wong for their help with Gaussian 09. WG was financially supported by a J.L. Stewart scholarship and a Curtis-Gordon scholarship.

Appendix A. Supplementary data

Supplementary data associated with this article can be found, in the online version, at http://dx.doi.org/10.1016/j.jphotochem.2014.01.012.

References

[1] N. Hoshino, Liquid crystal properties of metal–salicylaldimine complexes. Chemical modifications towards lower symmetry, Coordination Chemistry Reviews 174 (1998) 77.
[2] J. Zhao, B. Zhao, J. Liu, W. Xu, Z. Wang, Spectroscopy study on the photochromism of Schiff Bases N,N′-bis(salicylidene)-1,2-diaminoethane and N,N′-bis(salicylidene)-1,6-hexanediamine, Spectrochimica Acta Part A: Molecular and Biomolecular Spectroscopy 57 (2001) 149.
[3] G. Türkoğlua, H. Berber, H. Dal, C. Öğretirb, Synthesis, characterization, tautomerism and theoretical study of some new Schiff base derivatives, Spectrochimica Acta, Part A 79 (2011) 1573.
[4] J.L. Serrano, Metallomesogens: Synthesis, Properties, and Applications, VCH, Weinheim, 1996.
[5] R. Paschke, S. Liebsch, C. Tschierske, M.A. Oakley, E. Sinn, Synthesis and mesogenic properties of binuclear copper(II) complexes derived from salicylaldimine schiff bases, Inorganic Chemistry 42 (2003) 8230.
[6] C.V. Yelamaggad, R. Prabhu, G. Shanker, D.W. Bruce, Optically active, mesogenic lanthanide complexes: design, synthesis and characterization, Liquid Crystals 36 (2009) 247.
[7] R. Van Deun, K. Binnemans, Mesomorphic lanthanide complexes with azomethine ligands, Journal of Alloys and Compounds 303–304 (2000) 146.
[8] D. Lopez de Murillas, R. Pinol, M. Blanca Ros, J.L. Serrano, T. Sierra, M. Rosario de la Fuente, Structure–activity studies of ferroelectric and antiferroelectric imine ligands and their palladium(II) complexes. An antiferroelectric metallomesogen, Journal of Materials Chemistry 14 (2004) 1117.
[9] M.J. Frisch, G.W. Trucks, H.B. Schlegel, G.E. Scuseria, M.A. Robb, J.R. Cheeseman, G. Scalmani, V. Barone, B. Mennucci, G.A. Petersson, H. Nakatsuji, M. Caricato, X. Li, H.P. Hratchian, A.F. Izmaylov, J. Bloino, G. Zheng, J.L. Sonnenberg, M. Hada, M. Ehara, K. Toyota, R. Fukuda, J. Hasegawa, M. Ishida, T. Nakajima, Y. Honda, O. Kitao, H. Nakai, T. Vreven, J. Montgomery, J.E. Peralta, F. Ogliaro, M. Bearpark, J.J. Heyd, E. Brothers, K.N. Kudin, V.N. Staroverov, R. Kobayashi, J. Normand, K. Raghavachari, A. Rendell, J.C. Burant, S.S. Iyengar, J. Tomasi, M. Cossi, N. Rega, J.M. Millam, M. Klene, J.E. Knox, J.B. Cross, V. Bakken, C. Adamo, J. Jaramillo, R. Gomperts, R.E. Stratmann, O. Yazyev, A.J. Austin, R. Cammi, C. Pomelli, J.W. Ochterski, R.L. Martin, K. Morokuma, V.G. Zakrzewski, G.A. Voth, P. Salvador, J.J. Dannenberg, S. Dapprich, A.D. Daniels, Ö. Farkas, J.B. Foresman, J.V. Ortiz, J. Cioslowski, D.J. Fox, Gaussian 09, Revision B.01 ed., Gaussian, Inc., Wallingford, 2009.
[10] Y.P. Tong, S.L. Zheng, Synthesis, structure, spectroscopic properties, DFT and TDDFT investigations of copper(II) complex with 2-(2-hydroxyphenyl)benzimidazole, J. Mol. Struct. 841 (2007) 34.
[11] E.D. Glendening, A.E. Reed, J.E. Carpenter and F. Weinhold, NBO, Version 3.

[12] H.H. Hammud, A. Ghannoum, M.S. Masoud, Spectral regression and correlation coefficients of some benzaldimines and salicylaldimines in different solvents, Spectrochimica Acta Part A: Molecular and Biomolecular Spectroscopy 63 (2006) 255.
[13] C.R. Bhattacharjee, G. Das, P. Mondal, Liquid-crystalline oxovanadium(IV) complexes accessed from bidentate [N, O] donor salicylaldimine Schiff-base ligands, Journal of Coordination Chemistry 64 (2012) 3273.
[14] R. Vafazadeh, V. Hayeri, A.C. Willis, Synthesis, crystal structure and electronic properties of bis(N-2-bromophenyl-salicydenaminato)copper(II) complex, Polyhedron 29 (2010) 1810.
[15] E. Tas, A. Kilic, N. Konak, I. Yilmaz, The sterically hindered salicylaldimine ligands with their copper(II) metal complexes: synthesis, spectroscopy, electrochemical and thin-layer spectroelectrochemical features, Polyhedron 27 (2008) 1024.